

Efficient method for the determination of extreme-ultraviolet optical constants in reactive materials: application to scandium and titanium

Yu. A. Uspenskii

Lebedev Physical Institute, Leninski prospekt 53, 117924 Moscow, Russia

John F. Seely

Naval Research Laboratory, Space Science Division, Washington, D.C. 20375

N. L. Popov and A. V. Vinogradov

Lebedev Physical Institute, Leninski prospekt 53, 117924 Moscow, Russia

Yu. P. Pershin and V. V. Kondratenko

Kharkiv State Polytechnic University, 21 Frunze street Kharkiv 310002, Ukraine

Received April 18, 2003; revised manuscript received September 12, 2003; accepted October 14, 2003

The chemical reaction of a sample with atmospheric gases causes a significant error in the determination of the complex refractive index $n = 1 - \delta + i\beta$ in the extreme-ultraviolet region. The protection of samples removes this effect but hampers the interpretation of measurements. To overcome this difficulty, we derive the exact dependences on film thickness of the reflectivity and transmissivity of a protected film. These dependences greatly simplify the determination of δ and β when the spectra of several films with different thickness and identical protection are measured. They also allow the verification of the $\delta(\omega)$ obtained from the Kramers–Kronig relation and even make the Kramers–Kronig method unnecessary in many cases. As a practical application, the optical constants of Sc and Ti are determined at $\hbar\omega = 18\text{--}70\text{ eV}$ and $18\text{--}99\text{ eV}$, respectively. The essential feature of our experimental technique is deposition of a film sample directly on a silicon photodiode that allows easy operation with both thin ($\sim 10\text{-nm}$) and thick ($\sim 100\text{-nm}$) films. The comparison of calculated reflectivities of Si–Sc multilayers with the measured values shows the high accuracy of the determined $\delta(\omega)$ and $\beta(\omega)$. © 2004 Optical Society of America

OCIS codes: 160.3900, 260.7200, 300.6560, 340.6720, 340.7480.

1. INTRODUCTION

Intensive studies of the optical constants $\delta(\omega)$ and $\beta(\omega)$ in the extreme-ultraviolet (EUV) region are motivated by numerous applications: EUV lithography, x-ray astrophysics, EUV lasers, attosecond metrology, etc. Despite the existence of various methods (reflectometry, ellipsometry, interferometry, transmission, and photoelectric yield measurements), accurate determination of $\delta(\omega)$ and $\beta(\omega)$, especially at long EUV wavelengths, still has significant difficulties. They are caused by the strong EUV absorption of C, N, and O atoms and the high sensitivity of $\delta(\omega)$ and $\beta(\omega)$ to the reaction of samples with atmospheric gases. These difficulties grow manifold and become of principal importance when reactive or getter materials such as alkalis, rare-earth elements, actinide metals, or most of the transition metals are investigated.

To exclude the effect of atmospheric gases, researchers have successfully performed the deposition and measurement of film samples under vacuum, without exposure to the atmosphere.¹ But this method requires an expensive setup and therefore is not often applied. In consideration of this problem, the EUV probe of a sample purity and the

correction of optical constants to take into account a thin oxide layer were suggested.^{2,3} The other approach to the problem is connected with the use of protected samples. The measurement and interpretation of angle-dependent reflectivity $R(\theta)$ isolate the contribution from a studied material and provide its δ and β .^{4,5} This procedure requires a simultaneous determination of the parameters of the capping and buffer layers as well as of the interfaces. For this reason, the accuracy of δ and β depends essentially on knowledge of the structure and composition of these layers and interfaces. The measurement and interpretation are rather laborious, as repetition at all ω of interest is necessary.

An alternative approach, which is based on transmission measurements of identically protected free-standing films of different thickness, was used by several authors.^{6,7} By use of the principle that identical protection does not affect the ratio of the transmissivities of the films, $\beta(\omega)$ was found from the measured spectra. The determination of $\delta(\omega)$ implied the use of the Kramers–Kronig relation, that is, knowledge of $\beta(\omega)$ in a wide frequency region. Problems arise in high-absorption inter-

vals, in which difficult fabrications of free-standing films of ~ 10 nm or thinner are required.

The present paper also utilizes the measurements of identically protected films of different thickness, but places them on silicon photodiodes. This modification makes possible the study of both thin and thick films, so that the determination of $\beta(\omega)$ in high- and low-absorption ranges can be done with equal ease. To lay the theoretical foundation to this method, we derive equations for the reflectivity and transmissivity of a protected film as functions of its thickness. The equations allow the determination of both $\delta(\omega)$ and $\beta(\omega)$ from the measured ratios of the reflectivities and transmissivities of identically protected films even without the Kramers–Kronig relation.

To test this method, we applied it to the determination of the EUV optical constants of Sc and Ti. Both metals are of practical interest for EUV optics. Scandium has been used successfully for fabrication of high-quality multilayer mirrors at the wavelengths 40–50 nm.^{8–10} Despite this fact, the $\delta(\omega)$ and $\beta(\omega)$ of Sc remain practically unknown, excluding the information obtained from first-principle calculations.¹¹ It is expected that the optical constants of Ti are similar to those of Sc but are shifted to higher photon energies. This means that Ti can become a promising candidate for fabrication of multilayer mirrors working at higher EUV frequencies, if the determination of the optical constants supports this expectation.

2. DERIVATION OF THE BASIC FORMULAS

The layered structure considered here consists of a capping structure C, a homogeneous layer of material being studied M, and a buffer structure B deposited on a substrate S. Its refraction-index profile, which is diagrammed in Fig. 1, includes a vacuum region with $n(z) = 1$ at $z < z_1$, the M layer with a complex refraction index $n(z) = n$ at $z_2 < z < z_3$ ($z_3 - z_2 = d$), and the substrate region with $n(z) = n_S$ at $z > z_4$. To derive the formulas for the reflection and transmission of the total structure, we find it convenient to decompose it into two parts: (1) the C structure sandwiched between the vacuum and M regions and (2) the B structure placed between the M and substrate regions. In the first part, two independent solutions for the electric field are

$$U_+(z) = \begin{cases} \exp[ik_0(z - z_1)p_V] + r_+ \exp[-ik_0(z - z_1)p_V], & z < z_1 \\ t_+ \exp[ik_0(z - z_2)p], & z > z_2 \end{cases}, \quad (1)$$

$$U_-(z) = \begin{cases} t_- \exp[-ik_0(z - z_1)p_V], & z < z_1 \\ \exp[-ik_0(z - z_2)p] + r_- \exp[ik_0(z - z_2)p], & z > z_2 \end{cases}, \quad (2)$$

with $k_0 = \omega/c = 2\pi/\lambda$, $p_V = \cos \theta_0$, $p = p' + ip'' = (n^2 - \sin^2 \theta_0)^{1/2}$, and θ_0 is the angle of incidence from vacuum. Here r_{\pm} are the complex reflection amplitudes from the C structure deposited on M for radiation going from vacuum to M or back. The quantities t_{\pm} are the respective transmission amplitudes.

In the second part, corresponding solutions are

$$V_+(z) = \begin{cases} \exp[ik_0(z - z_3)p] + \rho_+ \exp[-ik_0(z - z_3)p], & z < z_3 \\ \tau_+ \exp[ik_0(z - z_4)p_S], & z > z_4 \end{cases}, \quad (3)$$

$$V_-(z) = \begin{cases} \tau_- \exp[-ik_0(z - z_3)p], & z < z_3 \\ \exp[-ik_0(z - z_4)p_S] + \rho_- \exp[ik_0(z - z_4)p_S], & z > z_4 \end{cases}, \quad (4)$$

with $p_s = (n_s^2 - \sin^2 \theta_0)^{1/2}$. In these equations, the complex amplitudes of reflection (transmission) from (through) B deposited on S for radiation going from M or back are denoted as ρ_{\pm} and τ_{\pm} .

For the total structure, an electric field is tried in the form

$$E(z) = \begin{cases} A_+ U_+(z) + A_- U_-(z), & z < z_1 \\ A_+ U_+(z) + A_- U_-(z) = B_+ V_+(z) + B_- V_-(z), & z_2 < z < z_3 \\ B_+ V_+(z) + B_- V_-(z), & z > z_4 \end{cases}, \quad (5)$$

After the substitution of expressions for $U_{\pm}(z)$ and $V_{\pm}(z)$, Eq. (5) becomes

$$E(z) = \begin{cases} \exp[ik_0(z - z_1)p_V]A_+ + \exp[-ik_0(z - z_1)p_V](r_+A_+ + t_-A_-), & z < z_1 \\ \exp[ik_0(z - z_2)p]W_+ + \exp[-ik_0(z - z_2)p]W_-, & z_2 < z < z_3 \\ \exp[ik_0(z - z_4)p_S](B_+\tau_+ + B_-\rho_-) + \exp[-ik_0(z - z_4)p_S]B_-, & z > z_4 \end{cases}, \quad (6)$$

with

$$W_+ = A_+ t_+ + A_- r_- = B_+ \exp(-ik_0 p d), \\ W_- = A_- = (B_+ \rho_+ + B_- \tau_-) \exp(ik_0 p d). \quad (7)$$

The solution of interest to us is proportional to $\exp[ik_0(z - z_4)p_S]$ at $z > z_4$, that is, has $B_- = 0$. With this condition, it is easy to find from Eqs. (7)

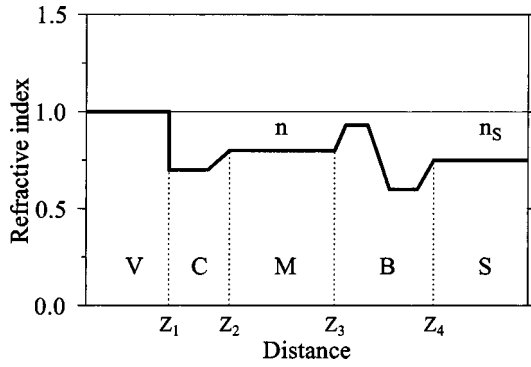


Fig. 1. Schematic representation of the refractive-index profile $n(z)$ in the protected layered structure under consideration. Vacuum and substrate regions are labeled V and S, a material under study is marked as M, and capping and buffer structures are symbolized by C and B.

$$A_-/A_+ = \frac{t_+\rho_+ \exp(2iD)}{1 - r_-\rho_+ \exp(2iD)},$$

$$B_+/A_+ = \frac{t_+ \exp(iD)}{1 - r_-\rho_+ \exp(2iD)}, \quad (8)$$

where $D = D' + iD'' = k_0 p d$. The complex reflection and transmission amplitudes of the total structure r and t may be calculated from Eq. (6) as $r = r_+ + t_- A_-/A_+$ and $t = \tau_+ B_+/A_+$. Using Eqs. (8), we arrive at the final expressions:

$$r = r_+ + \frac{t_+ t_- \exp(2iD) \rho_+}{1 - r_-\rho_+ \exp(2iD)}, \quad (9)$$

$$t = \frac{t_+ \tau_+ \exp(iD)}{1 - r_-\rho_+ \exp(2iD)}. \quad (10)$$

It should be noted that structures C and B may be arbitrarily complicated. Hence Eqs. (9) and (10) describe the transmission and reflection of a general layered structure with a homogeneous layer of thickness d inside. The presented equations are physically transparent. They coincide with the analogous equations for one unprotected M layer deposited on S if the Fresnel reflection and transmission amplitudes of the interfaces are replaced by r_{\pm} , ρ_{\pm} , t_{\pm} , and τ_{\pm} . In the particular case of a three-layer structure, equations of this type have been derived in Ref. 12. We also note a resemblance between Eqs. (9) and (10) and expressions describing the reflection and transmission of a Fabry–Perot cavity.

With Eqs. (9) and (10), the reflectivity R and transmissivity T of the structure under study may be written as

$$R = R_c |1 + \xi f \exp(2iD)|^2, \quad (11)$$

$$T = T_c T_b |f \exp(iD)|^2, \quad (12)$$

where $R_c = |r_+|^2$, $T_c = |t_+|^2 |p/p_V|$, $T_b = |\tau_+|^2 |p_S/p|$, and $\xi = t_+ t_- \rho_+ / r_+$. The factor $f = [1 - r_-\rho_+ \exp(2iD)]^{-1}$ arises from the multiple reflection of radiation inside the M layer. In the EUV region, this reflection is small, at a level of 1% or less, so generally $f \approx 1$. The only exceptions are special structures de-

signed for maximal reflection. This simplification gives approximate formulas for the reflectivity and transmissivity of protected films,

$$R = R_c [1 + 2 \cos(2D' + \chi) |\xi| \exp(-2D'') + |\xi|^2 \exp(-4D'')], \quad (13)$$

$$T = T_c T_b \exp(-2D''), \quad (14)$$

which describe the effects of the capping and buffer layers with a minimal set of parameters: R_c , $T_{cb} = T_c T_b$, and $\xi = |\xi| \exp(i\chi)$. It should be stressed that all complications in the C and B structures (oxidized layers, barrier layers, mixed interfaces, etc.) manifest themselves only through changes in these parameters. This allows us to avoid a detailed study of the C and B structures if the parameters R_c , T_{cb} , and ξ are fitted.

The effect of roughness is not reduced entirely to changes in R_c , T_{cb} , and ξ . Though complete analysis of the rough C/M/B structure is rather complicated,¹³ this statement can be simply explained in the case of normal incidence. In this case, the oblique propagation of radiation arises only from scattering on roughness. It is convenient to divide the scattering processes into two groups. The first group includes the processes with the normal propagation inside the M layer. Oblique propagation takes place inside only the C or B region. The second group corresponds to the processes with oblique propagation inside the M region. It is evident that the processes of the first group change only parameters R_c , T_{cb} , and ξ while retaining the same exponential factor $\exp(iD)$ ($D = k_0 d n$). That is, in this case Eqs. (13) and (14) are untouched. The processes of the second group change the exponential factor to $\exp(iD_1)$ with $D_1 = k_0 d (n^2 - \sin^2 \theta_1)^{1/2}$, where θ_1 is the angle of oblique propagation inside the M region. In this (second) case, the effects of roughness change the dependences of R and T on d given by Eqs. (13) and (14). At long EUV wavelengths, where λ is much larger than the height of roughness, these corrections are small. But at short wavelengths, where roughness essentially affects R and T , the check of accuracy of Eqs. (13) and (14) is desirable.

3. SAMPLE PREPARATION AND MEASUREMENTS

The six films of Sc and the six of Ti were prepared by dc-magnetron sputtering at 3×10^{-3} Torr of Ar. All films were deposited on silicon photodiodes from International Radiation Detectors Inc. (of the type AXUV-SP2 for Sc and AXUV-100 for Ti) and capped with a silicon film of 5 nm (Sc) and 8 nm (Ti). The photodiodes were fabricated by a lithographic process and had a SiO₂ dead layer of 6-nm thickness at the surface. Previous studies indicated that photodiodes from the same batch have identical sensitivities within the experimental uncertainty of a few percent. For Sc films the thickness was 7.5, 10, 12.5, 70, 100, and 130 nm, and for Ti it was 10, 14, 18, 40, 70, and 100 nm. A classification of the films of both metals as thin (~ 10 nm) and thick (~ 100 nm) was caused by the existence of high- and low-absorption intervals inside the EUV region of interest, which dictated a combined use of thin and thick films, as discussed below. Preliminary es-

timation of d was based on deposition time and the measured rate of deposition. Obtained quantities were subsequently checked with the reflection of Cu- K_α radiation. These measurements as well as our previous experience showed that the accuracy of d was approximately 1%, and its variation across the film surface was of the order of 0.5%.

The transmissivity of all Sc films and the reflectivity of the Sc films with $d = 7.5, 10, 12.5,$ and 100 nm were measured in the photon-energy interval of 18–70 eV. The transmissivity of Ti films was measured in the wider interval of 18–99 eV. The measurements were performed with the National Synchrotron Light Source beamline X24C at Brookhaven National Laboratory. The radiation was dispersed by a monochromator with 600 resolving power. Thin beamline filters passed the wavelengths of interest and attenuated the higher-harmonic radiation from the monochromator. The part of the higher-harmonic radiation was approximately 1%, as has been found from the transmission grating measurements of the spectral content of the beam. The radiation beam was 2 mm in diameter and was incident normal to the surfaces of the photodiodes. The coated photodiodes were moved sequentially into the radiation beam, and the incident wavelength λ was scanned under computer control. At each wavelength step, the current resulting from the reflected or transmitted beam was normalized by the current from an uncoated photodiode of the same type inserted in the direct beam. The respective current ratios represented the reflectivity and transmittivity of the coating.

4. DETERMINATION OF OPTICAL CONSTANTS AND DISCUSSION OF RESULTS

The measured transmissivity of Sc and Ti films is shown in Fig. 2. It can be seen that both metals have low transmission in the interval of intense $3p \rightarrow 3d$ electron transitions (the region of the M_3 edge), which is placed at 28–52 eV in Sc and at 32–61 eV in Ti. In this interval a EUV signal transmitted through thick films is so weak that it is comparable to the small amount of higher harmonic radiation, which is weakly attenuated in the films. The increase of $T(\omega)$ imitated by the higher harmonic radiation is very significant (100% of the EUV signal), and therefore only thin films provide the true $T(\omega)$ when absorption is high. Out of this interval, the attenuation of a EUV signal transmitted through thin samples is low and controlled mainly by the capping layer and the detector dead layer. Variations in the thickness of these layers strongly affect the results, so in low-absorption intervals the most precise data are obtained with thick films. These reasons defined our choice of the sample thicknesses and selection of reliable experimental data for the determination of $\beta(\omega)$.

As follows from Eq. (14), the ratio of transmissivities of two films with identical C and B structures directly determines $\beta(\omega)$ when radiation propagates normal to the surface ($p'' = \beta$):

$$\beta(\omega) = \frac{1}{2k_0(d_j - d_i)} \ln[T_i(\omega)/T_j(\omega)], \quad (15)$$

where d_i, d_j are the thicknesses of the films and $T_i(\omega), T_j(\omega)$ are their respective transmissivities. To minimize the errors arising from higher harmonic radiation and small variations in the C and B structures, which have been discussed above, we made a special selection of film pairs for the determination of $\beta(\omega)$. That is, we assumed that a transmitted signal should be three times larger than a signal from the higher harmonic radiation, which produced $d_i, d_j < 0.2\lambda/\beta(\omega)$. Since the relative variations of thickness in the C and B structures are of the order of 10%, we estimated that the difference $|d_i - d_j|$ should be larger than $0.1\lambda/\beta(\omega)$. These empirical criteria were used to select film pairs (different along the studied wavelength interval) for the calculation of β from Eq. (15). The resulting $\beta(\omega)$ of Sc is presented in Fig. 3. The inset demonstrates good agreement between β 's found from several pairs of Sc films in high- and low-absorption intervals. This agreement shows that the protection of samples is practically identical, and the corrections to Eq. (15) caused by multiple reflection and roughness, which were discussed in Section 2, are small.

Our measurements of $\beta(\omega)$ were performed in a wide energy range, which included the interval of highest EUV absorption. In view of this, the use of the Kramers–Kronig method for the determination of $\delta(\omega)$ was quite

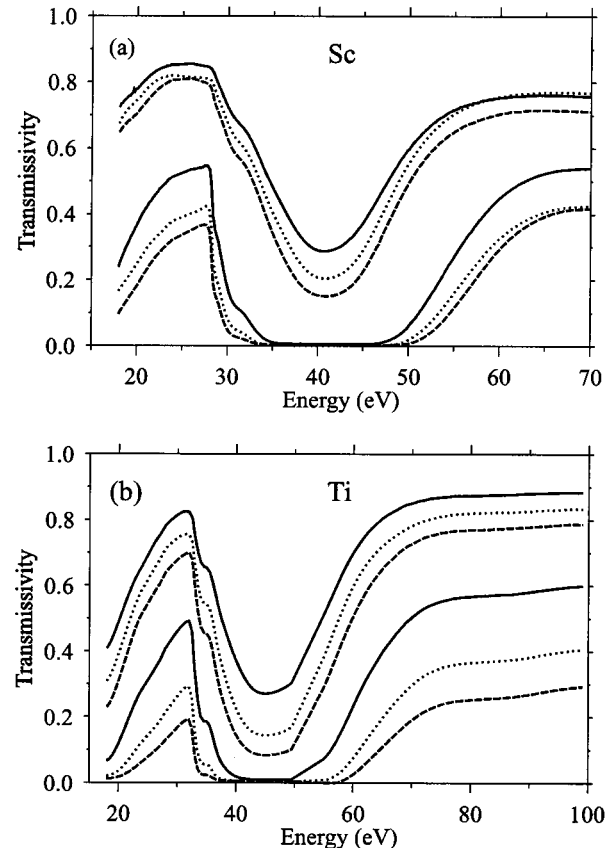


Fig. 2. Transmissivity spectra of Sc and Ti (a) for Sc films with thickness $d = 7.5, 10, 12.5, 70, 100,$ and 130 nm (going from the top down) and (b) for Ti films with $d = 10, 14, 18, 40, 70,$ and 100 nm.

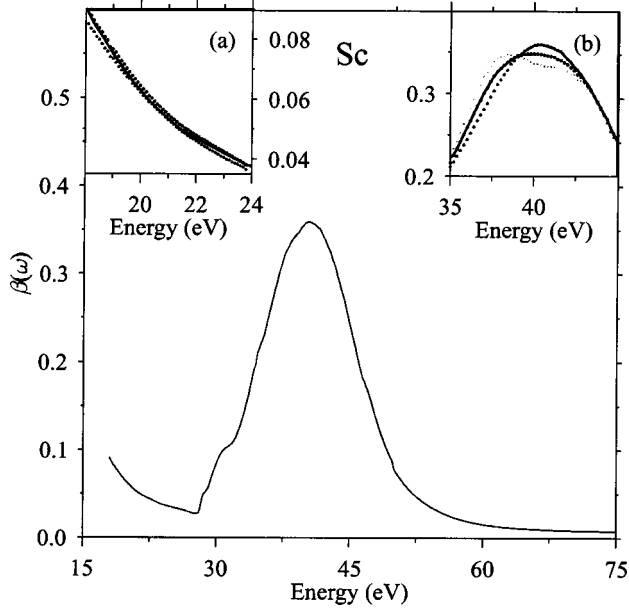


Fig. 3. Net $\beta(\omega)$ of Sc found from Eq. (15). Insert (a) shows agreement between this $\beta(\omega)$ (solid curve) and the values obtained from the films pairs of 7.5–130, 10–100, and 12.5–100 nm (symbols) in the low-absorption region of 18–24 eV. Insert (b) demonstrates the agreement of the $\beta(\omega)$ with the results found for the film pairs 7.5–10, 7.5–12.5, and 10–12.5 nm in the high-absorption region of 35–45 eV.

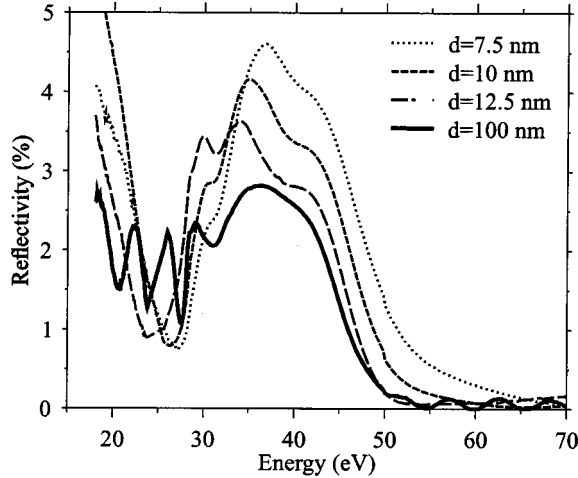


Fig. 4. Reflectivity spectra for Sc films of different thickness.

justified. To apply this method, we supplemented the measured $\beta(\omega)$ by the calculated results of Ref. 11 at $\hbar\omega < 18$ eV and the data of the atomic tables¹⁴ at $\hbar\omega > 70$ eV (Sc) or 99 eV (Ti). The discontinuity of $\beta(\omega)$, which was caused by imperfect consistency of data from different origins, was removed by a smooth interpolation of the supplementary $\beta(\omega)$'s to our results in the intervals of 2 eV at $\hbar\omega < 18$ eV and of 20 eV at $\hbar\omega > 70$ or 99 eV. The $\delta(\omega)$ obtained with the Kramers–Kronig method, as well as $\beta(\omega)$, were then refined by an iterative procedure in which the multiple-reflection factor $f(\omega)$ [see Eq. (12)] was included.

Since the Kramers–Kronig calculation invoked the data of other studies, a question of its accuracy arises. As will be seen later, the analysis of reflectivity spectra

provides a good check of these results. Figure 4 shows the measured reflectivity of Sc films with $d = 7.5, 10, 12.5,$ and 100 nm. The reflectivities of thin films are rather smooth and similar in appearance, whereas the $R(\omega)$ of the thick film ($d = 100$ nm) has oscillations in the high-transparency intervals. These oscillations arise from the interference of EUV waves reflected from the C and B structures and are described by the term proportional to $\cos(2D' + \chi)\{D' = d[1 - \delta(\omega)]\omega/c\}$ in Eq. (13). That is, the period of these oscillations depends directly on $\delta(\omega)$ and d . This fact may be used to check $\delta(\omega)$ or even to determine it if $R(\omega)$ is measured on a series of films with varied thicknesses.

According to Eq. (13), the ratio of the normal incidence reflectivities of two films with identical C and B structures is

$$\begin{aligned} R_i(\omega)/R_j(\omega) &= \frac{1 + 2 \cos(2D_i' + \chi)|\xi|\exp(-2D_i'') + |\xi|^2 \exp(-4D_i'')}{1 + 2 \cos(2D_j' + \chi)|\xi|\exp(-2D_j'') + |\xi|^2 \exp(-4D_j'')}, \end{aligned} \quad (16)$$

where $\xi = \xi(\omega) = |\xi|\exp(i\chi)$, $D_i = D_i' + iD_i'' = k_0 d_i [1 - \delta(\omega) + i\beta(\omega)]$, and d_i and d_j are the film thicknesses. The right-hand side of Eq. (16) depends on three parameters: δ , $|\xi|$, and χ (d_i , d_j , and β are assumed to be known). These parameters may be found at each ω by fitting to experimental values $R_i(\omega)/R_j(\omega)$, if the reflectivity of five or more films (four or more thick films among them) was measured. Our simulation supported this idea and showed that this procedure is stable to experimental errors. A limit of time at the synchrotron beamline did not allow the realization of this program at full length. Nevertheless, with the measurements of $R(\omega)$ for the three thin films and one thick film of Sc, we were able to check the $\delta(\omega)$ of Sc found from the Kramers–Kronig method and even correct it somewhat.

To find this correction, we denote the difference between the true and our supplementary $\beta(\omega)$ as $\Delta\beta(\omega)$. Using the Kramers–Kronig relation, we can easily obtain correction to $\delta(\omega)$:

$$\begin{aligned} \Delta\delta(\omega) &= \int_0^{\omega_{\min}} \frac{2\omega' \Delta\beta(\omega')}{\omega'^2 - \omega^2} d\omega' + \int_{\omega_{\max}}^{\infty} \frac{2\omega' \Delta\beta(\omega')}{\omega'^2 - \omega^2} d\omega' \\ &\approx -\frac{1}{\omega^2} \int_0^{\omega_{\min}} 2\omega' \Delta\beta(\omega') d\omega' \\ &\quad + \int_{\omega_{\min}}^{\infty} 2\Delta\beta(\omega')/\omega' d\omega' \\ &\equiv -\delta f/\omega^2 + \Delta, \end{aligned} \quad (17)$$

where ω is assumed to be in the interval of measurements $\omega_{\min} < \omega < \omega_{\max}$ and the approximations $\omega \gg \omega'$ and $\omega \ll \omega'$ were used to estimate, respectively, the first and the second integrals. Both constants δf and Δ , which determine $\Delta\delta(\omega)$, can be obtained by fitting the calculated ratios $R_i(\omega)/R_j(\omega)$ to experimental quantities. To do this calculation, we modeled all samples by the layered structure of SiO_2 (2 nm), Si (3 nm), Sc (d), SiO_2 (6 nm), and Si with a varied thickness d and the ideal interfaces. The

resulting δf was 2.5 eV^2 , which corresponds to a missing oscillator strength 0.1 at $\hbar\omega < 18 \text{ eV}$, and Δ was negligibly small. These corrections were included in $\delta(\omega)$, which is shown in Fig. 5. As reflectivity measurements were not performed for Ti, the same values of δf and Δ were used for this metal. The fit of the calculated ratio $R_i(\omega)/R_j(\omega)$ ($d_i = 100 \text{ nm}$, $d_j = 7.5 \text{ nm}$) for Sc to the experimental one is shown in Fig. 6. It can be seen that both calculated and experimental values identically oscillate with ω , indicating the high accuracy of the determined $\delta(\omega)$. The amplitudes of oscillations are slightly different. This difference arises from the existence of a mixed Si–Sc region of 3-nm width⁹ and other features of the capping and buffer layers and the interfaces that were not accounted for in the calculation. These features are perfectly canceled out from Eq. (15) but remain in Eq. (16) owing to $\xi(\omega)$. Our computational experience shows, however, that the existence of a mixed region as well as many other (often uncontrollable) details of actual interface structures do not practically affect the period of oscillations of $R_i(\omega)/R_j(\omega)$. This allows us to fit $\delta(\omega)$ by using a rather simple interface model, as was done above for the Sc samples. Moreover, in the case of sufficient experimental data for reflectivity ratios, the complex value $\xi(\omega)$ can be fitted in a way that fully excludes the need for detailed information on interface structure.

It is of interest to compare our results with optical constants from the atomic tables,¹⁴ which are also presented in Fig. 5. For Sc, the data agree well at low and high en-

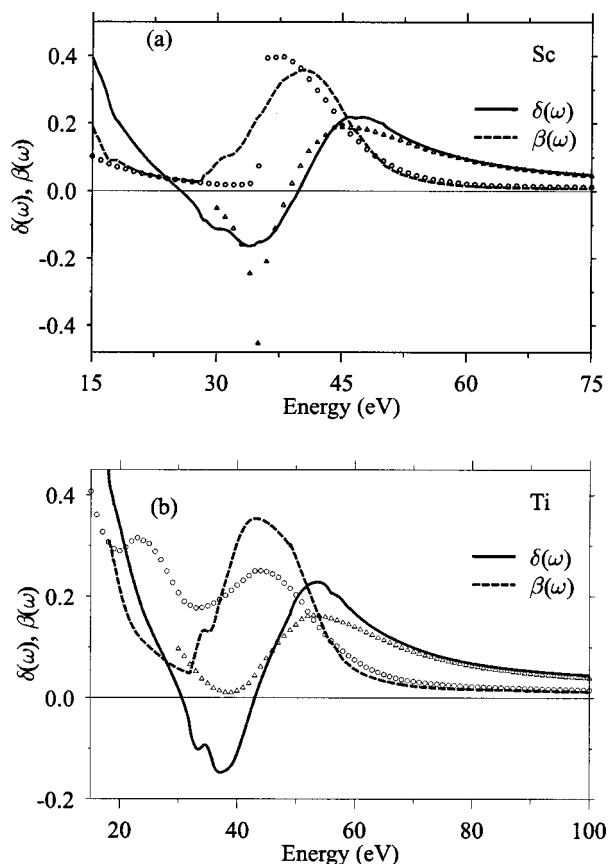


Fig. 5. Calculated optical constants $\delta(\omega)$ and $\beta(\omega)$ (curves) in comparison with the atomic tables data (symbols): (a) Sc and (b) Ti.

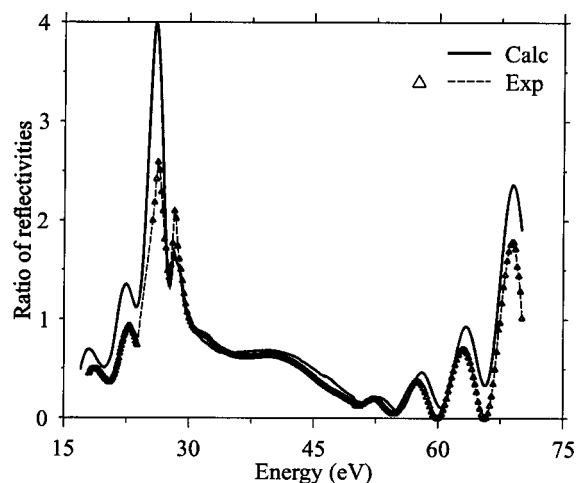


Fig. 6. Calculated and experimental reflectivity ratios $R_i(\omega)/R_j(\omega)$ for $d_i = 100 \text{ nm}$ and $d_j = 7.5 \text{ nm}$.

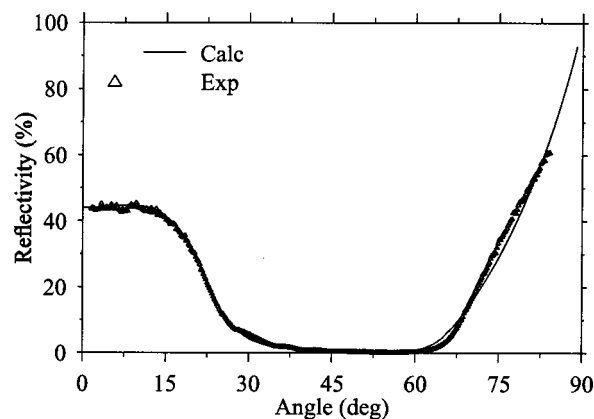


Fig. 7. Calculated and experimental angle-dependent reflectivity of the Si (15-nm)/Sc (12-nm) multilayer at $\lambda = 46.9 \text{ nm}$.

ergies, whereas for Ti a close agreement is observed only at high energies. In the vicinity of the M edge, our constants are rather different from those of Ref. 14, especially for Ti. Similar disagreement takes place for Ti at low energies. It looks probable that the maximum of $\beta(\omega)$ in Ti at 23 eV and too-high values of this quantity below 32 eV, which were cited in the atomic tables, have actually arisen from the contamination of samples by N and O atoms having the highest EUV absorption at $\hbar\omega \approx 20 \text{ eV}$.¹⁴

Our optical constants of Sc were also verified by the calculation of reflectivity spectra for several Si–Sc multilayers experimentally studied in Refs. 9, 10, and 15. In all multilayers the number of layers was 10 and the roughness $\sigma = 0.3 \text{ nm}$ was assumed. Figure 7 compares the calculated angle-dependent reflectivity $R(\theta)$ of a Si (15-nm)/Sc (12-nm) multilayer at $\hbar\omega = 26.4 \text{ eV}$ with the experimental result of Ref. 15. Figure 8 demonstrates agreement between the calculated and the measured⁹ reflectivities for two multilayers: (1) Si (10.9 nm) and Sc (8.6 nm) and (2) Si (14.8 nm) and Sc (11.6 nm). For the former multilayer, the result of calculation with the optical constants of Sc obtained from the atomic tables¹⁴ is also shown for comparison. Last, Fig. 9 shows the calcu-

lated and experimental energy-dependent reflectivities of the thermally stable Si (7.3-nm), W (0.6-nm), Sc (10.9-nm), and W (0.6-nm) multilayer designed for the maximal reflection at $\hbar\omega = 31$ eV.¹⁰ All these examples confirm the high accuracy of our $\delta(\omega)$ and $\beta(\omega)$.

A comparative analysis of the optical constants of Sc and Ti reveals some trends in their behavior. Both met-

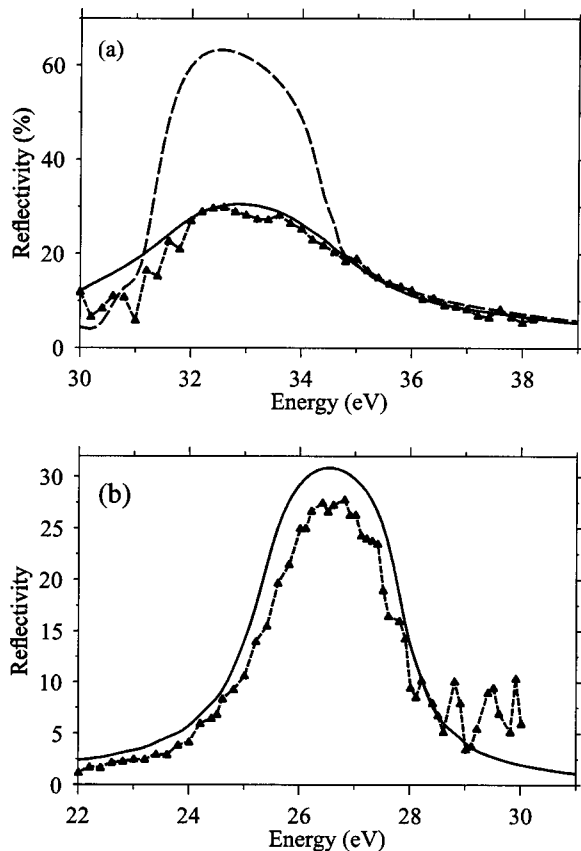


Fig. 8. Calculated (solid curve) and experimental (curve with symbols) normal-incidence reflectivity spectra of (a) the Si (10.9-nm) and Sc (8.6-nm) multilayer (the dashed curve shows the result of calculation with optical constants of Sc from Ref. 14) and (b) the Si (14.8-nm) and Sc (11.6-nm) multilayer.

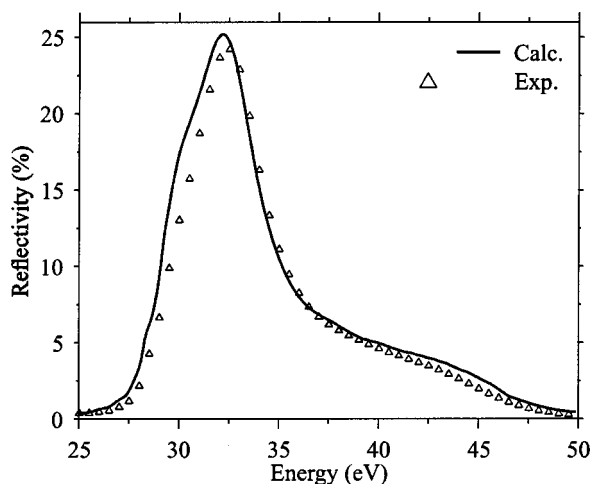


Fig. 9. Calculated (solid curve) and measured (symbols) normal-incidence reflectivity of the Si (7.3-nm), W (0.6-nm), Sc (10.9-nm), and W (0.6-nm) multilayer.

als have a similar distribution of $3p \rightarrow 3d$ electron transitions with the total oscillator strength of ~ 4.2 , which manifests itself in analogous dependences $\beta(\omega)$. Because of the larger nuclear charge, Ti has a deeper $3p$ level than Sc has and, respectively, a higher energy of the $3p \rightarrow 3d$ transitions, which start at 32 eV compared with 28 eV in Sc. A smaller atomic volume of Ti, which is only 0.7 the volume of Sc, leads to a significantly wider $3d$ band of Ti and to a larger interval of intense $3p \rightarrow 3d$ excitations as compared with Sc. Higher atomic density and a larger number of valence electrons of Ti dictate its significantly higher (1.7 times) EUV absorption below the M edge compared with Sc. Analogous trends in the spectra of transition metals have been derived in Refs. 11 and 16 from the analysis of *ab initio* EUV calculations for the $3d$ and $4d$ transition metals.

These trends allow a comparison of the potentials of Sc and Ti for the fabrication of good multilayer reflectors. A lower EUV absorption and a lower value of $\delta(\omega)$ (the latter is caused by the lower energy of its M edge) make Sc preferable at $\hbar\omega < 28$ eV. This estimation correlates well with the measured high performance of Si/Sc multilayer mirrors reported in Refs. 8, 9, and 15. But at $\hbar\omega = 28$ –33 eV, these advantages accrue to Ti, which is a good candidate for fabrication of high-reflecting multilayer mirrors working at these energies. One more metal that is promising for the design of EUV mirrors is Mg.¹⁷ At long wavelengths, it has low EUV absorption and a low value of $\delta(\omega)$, resulting from the intense L_3 edge at $\hbar\omega = 49.5$ eV. Recent fabrication of high-reflective and high-polarizing multilayers that use Mg¹⁸ attracted significant attention to this element. In this connection, it would be interesting to apply the present method to Mg, giving special attention to the vicinity of the L_3 edge, despite the fact that several measurements of Mg below its L edge have been made (see Ref. 6 and references therein).

5. CONCLUSIONS

The experimental and theoretical innovations of the present method eliminate the problems with air contamination and make possible the determination of EUV optical constants of reactive and getter materials. The examples given indicate that the obtained $\delta(\omega)$ and $\beta(\omega)$ are accurate within a few percent. The experimental method is simple to use and does not require an expensive experimental setup. In the intervals of high and moderate transparency, the direct determination of the index of refraction without the Kramers–Kronig relation is possible. In this respect, the potentials of the method approach those of the direct measurement of $\delta(\omega)$ with a novel EUV interferometer¹⁹ but with the additional beneficial exclusion of the effects of air contamination and the requirement of free-standing films for experiments.

ACKNOWLEDGMENTS

The authors are thankful to R. Souffi for useful comments. This research was supported in part by U.S. Civilian Research and Development Foundation grants RP1-2267 and RP-2-2326-MO-02, as well as grant 2297 of

the International Science and Technology Center. Yu. A. Uspenskii, N. L. Popov, and A. V. Vinogradov were also supported by grants N 01-02-17432a, N 02-02-06644, N 02-02-16599-a, and N 03-02-16438-a of the Russian Fund for Basic Research. J. F. Seely was supported by NASA grant S-92543-F. Yu. A. Uspenskii is grateful to Tohoku University for its hospitality during the final stage of this research.

J. Seely, the corresponding author, can be reached by e-mail at john.seely@nrl.navy.mil.

REFERENCES

1. C. Tarrío, R. N. Watts, T. B. Lucatorto, J. M. Slaughter, and M. Falce, "Optical constants of *in situ*-deposited films of important extreme-ultraviolet multilayer mirror materials," *Appl. Opt.* **37**, 4100–4104 (1998).
2. R. M. Fechtchenko and A. V. Vinogradov, "Reflection from surfaces with a thin overlayer," *Opt. Lett.* **25**, 998–1000 (2000).
3. R. M. Fechtchenko, A. V. Popov, and A. V. Vinogradov, "On reflection from surfaces with a thin overlayer," *J. Russ. Laser Res.* **22**, 139–148 (2001).
4. R. Souffi and E. M. Gullikson, "Reflectance measurements on clean surfaces for the determination of optical constants of silicon in the extreme ultraviolet–soft-x-ray region," *Appl. Opt.* **36**, 5499–5507 (1997).
5. I. A. Artioukov, B. R. Benware, J. J. Rocca, M. Forsythe, Yu. A. Uspenskii, and A. V. Vinogradov, "Determination of XUV optical constants by reflectometry using a high-repetition rate 46.9-nm laser," *IEEE J. Sel. Top. Quantum Electron.* **5**, 1495–1501 (1999).
6. E. M. Gullikson, P. Denham, S. Mrowka, and J. H. Underwood, "Absolute photoabsorption measurements of Mg, Al, and Si in the soft-x-ray region below the $L_{2,3}$ edges," *Phys. Rev. B* **49**, 16283–16288 (1994).
7. R. Souffi and E. M. Gullikson, "Absolute photoabsorption measurements of molybdenum in the range 60–930 eV for optical constant determination," *Appl. Opt.* **37**, 1713–1719 (1998).
8. Yu. A. Uspenskii, V. E. Levashov, A. V. Vinogradov, A. I. Fedorenko, V. V. Kondratenko, Yu. P. Pershin, E. N. Zubarev, and V. Yu. Fedotov, "High-reflectivity multilayer mirrors for a vacuum-ultraviolet interval of 35–50 nm," *Opt. Lett.* **23**, 771–773 (1998).
9. Yu. A. Uspenskii, V. E. Levashov, A. V. Vinogradov, A. I. Fedorenko, V. V. Kondratenko, Yu. P. Pershin, E. N. Zubarev, S. Mrowka, and F. Schäfers, "Sc–Si normal incidence mirrors for a VUV interval of 35–50 nm," *Nucl. Instrum. Methods Phys. Res. A* **448**, 147–151 (2000).
10. J. F. Seely, Yu. A. Uspenskii, Yu. P. Pershin, V. V. Kondratenko, and A. V. Vinogradov, "Skylab 3600 groove/mm replica grating with a scandium–silicon multilayer coating and high normal-incidence efficiency at 38-nm wavelength," *Appl. Opt.* **41**, 1846–1851 (2002).
11. Yu. A. Uspenskii, S. V. Antonov, V. Yu. Fedotov, and A. V. Vinogradov, "Optical properties of 3D transition metals in the spectral interval of interest for discharge-pumped XUV lasers," in *Soft X-Ray Lasers and Applications II*, J. J. Rocca and L. B. Da Silva, eds., *Proc. SPIE* **3156**, 288–294 (1997).
12. Yu. A. Uspenskii and B. N. Harmon, "Large selective magneto-optic response from magnetic semiconducting layered structures," *Phys. Rev. B* **61**, R10571–R10574 (2000).
13. Yu. A. Uspenskii and A. V. Vinogradov (data available from the authors).
14. B. L. Henke, E. M. Gullikson, and J. C. Davis, "X-ray interaction: photoabsorption, scattering, transmission and reflection at $E = 10\text{--}30,000$ eV, $Z = 1\text{--}92$," *At. Data Nucl. Data Tables* **54**, 181–342 (1993).
15. J. J. Rocca, M. Frati, B. Benware, M. Seminario, J. Filevich, M. Marconi, K. Kanizay, A. Ozols, I. A. Artukov, A. Vinogradov, and Yu. A. Uspenskii, "Capillary discharge tabletop soft X-ray lasers reach new wavelengths and applications," *C. R. Acad. Sci. Paris Ser. IV* **1**, 1063–1072 (2000).
16. A. G. Nargizyan, S. N. Rashkeev, and Yu. A. Uspenskii, "Microscopic calculations of the optical properties of 4d-transition metals in the vacuum UV," *Sov. Phys. Solid State* **34**, 626–632 (1992).
17. E. Spiller, *Soft X-Ray Optics* (SPIE Optical Engineering Press, Bellingham, Wash., 1994).
18. Y. Hotta, N. Furudate, M. Yamamoto, and N. Watanabe, "Design and fabrication of multilayer mirrors for He-II radiation," *Surf. Rev. Lett.* **9**, 571–576 (2002).
19. C. Chang, E. Anderson, P. Naulleau, E. Gullikson, K. Goldberg, and D. Attwood, "Direct measurement of index of refraction in the extreme-ultraviolet wavelength region with a novel interferometer," *Opt. Lett.* **27**, 1028–1030 (2002).